Peierls instability and superconductivity in quasi-one-dimensional conductors

B. Horovitz*
The Racah Institute of Physics, The Hebrew University of Jerusalem, Jerusalem, Israel
(Received 16 August 1976)

The transition temperature of the Peierls phase (T_P) and of the superconducting phase (T_s) are studied, including a hopping-type interchain coupling and retardation effects due to finite bare phonon frequency ω_0. The interactions between the electrons include large and small momentum transfers with attractive couplings s_1, s_2, respectively. The set of most diverging diagrams is summed and the coexistence line (for which $T_P = T_s$) is shown to be $s_1 = 2s_2$ for the nonretarded interaction. For $s_1 \neq 2s_2$ the two phases exclude each other. For a finite ω_0, increasing ω_0 is shown to increase T_s while decrease T_P. Higher temperatures T_s are possible if (a) ω_0 is higher; (b) s_1, s_2 are stronger, but s_1 must stay below a critical value determined by s_2 and ω_0 (for $s_2 = 1$, $\max(T_s) \simeq \omega_0/20$); (c) the commensurate case is avoided; (d) the Peierls instability is suppressed, i.e., by a large enough interchain coupling. The dependence of T_P on ω_0 implies a positive isotope shift which is measurable if $\omega_0 \gtrsim 2\pi T_P$. Such high-frequency phonons are important for high-temperature superconductivity and the isotope shift provides a method for locating them in the Peierls phase.

I. INTRODUCTION

The search for high-temperature superconductors has motivated an extensive study of quasi-one-dimensional (1-D) conductors in the last few years.[1] The motivation is due to Fröhlich[2] and Little[3] for proposing 1-D models for superconductivity and to Weger[4] for demonstrating the 1-D nature of the intermetallic $A15$ compounds which may contribute to their high T_s.

Experimental studies involve mainly $K_2Pt(CN)_4Br_{0.3} \cdot 3H_2O$ (KCP)[5] with a Peierls instability at $T_P \simeq 110$ °K, tetrathiafulvalene–tetracyanoquinodimethane[6] (TTF-TCNQ) with $T_P = 53$ °K, and similar compounds of the TCNQ family.[7] The polymer $(SN)_x$ is a superconductor below $T_s = 0.33$ °K,[8] however, it is not clear if its quasi-1D nature is intrinsic or caused by its fibrous composition.[9]

Theoretically it was shown that summation of the most diverging diagrams in a strictly 1-D system[10] (parquet diagrams) leads to coexistence of superconductivity and the Peierls phase, and $T_P = T_s$. Since in a 1-D system an ordered phase can exist only at $T = 0$, more diagrams must be summed. Using second-order renormalization group the transition temperatures are lowered to $T = 0$,[11] but still the two phases coexist. However, the use of renormalization group for attractive interactions is questionable.[11] In particular, exact results[12] and mapping on the two-dimensional Coulomb gas[13] show that the two phases do not coexist in general.

To be more specific we introduce the important couplings as in Fig. 1. These couplings represent momentum transfer of $\sim 2p_F$ (g_1) where p_F is the Fermi momentum and transfer of small momentum $|q| \ll p_F$ (g_2). Also present are the umklapp scattering (g_3) and scattering involving electrons only on one side of the Fermi surface (g_4). We are interested mainly with the attractive interactions s_1, $s_2 > 0$,

$$s_1 = -g_1 N(0), \qquad s_2 = -g_2 N(0), \tag{1.1}$$

where $N(\epsilon)$ is the electron density of states for both spins, and $\epsilon = 0$ is the Fermi level.

The exact 1-D results[12,13] show that superconductivity and the Peierls phase coexist only near the line $s_1 = 2s_2$ and apart from that only one phase exists. The line $s_1 = 2s_2$ is a coexistence line in the sense that one of the response functions diverges stronger than the other as $T \to 0$ if $s_1 \neq 2s_2$.

In order to describe systems with finite transition temperatures we have to introduce an interchain coupling. The limit of small interchain coupling was investigated near the available exact 1-D results[14] or by using renormalization-group meth-

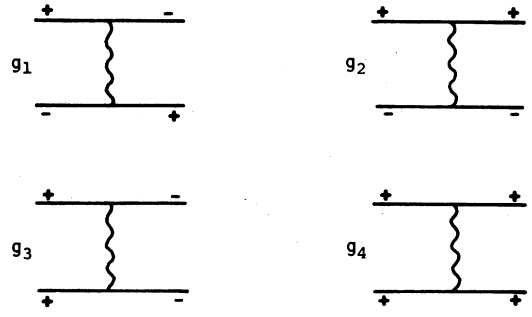

FIG. 1. Coupling constants for electron-electron scattering. Signs ± describe electrons with momenta $\sim \pm p_F$. In each diagram reversal of all signs is also possible.

ods.[15] If the electrons are restricted to move along the chains and there is a long-range interchain interaction, then it is possible to have $T_P \neq 0$, but superconductivity stays at $T_s = 0$.[14,15] The Peierls instability corresponds to charge-density waves (CDW's). The Coulomb interaction correlates the phases of these waves on different chains, and so $T_P \neq 0$. However, the phase of the superconducting state conjugates to the number of electrons. Thus interchain phase correlations can be achieved only by electron tunneling corresponding to a Josephson junction.

In what follows we deal only with interchain coupling due to electron tunneling between neighboring chains. This leads to the more interesting case with both T_P and T_s finite. For small interchain coupling it was shown[14] that near the special solutions[12] ($s_1 = 0$ or $s_1 = \frac{12}{5}$) the line $s_1 = 2s_2$ remains the coexistence line such that $T_P = T_s$ on this line.

The case of intermediate interchain coupling can be treated using mean-field (MF) theory.[16] We quote here the main results of Ref. 16 for the Peierls phase with $s_2 = 0$.

The electronic dispersion which describes electron hopping between adjacent chains is

$$\epsilon_{\vec{p}} = \epsilon(p_z) - 2t_\perp(\cos ap_x + \cos ap_y), \tag{1.2}$$

where $t_\perp$ is the transfer integral in the transverse x, y directions and a is the interchain distance.

The important property of Eq. (1.2) is that if $\epsilon(p_z)$ has electron hole symmetry,

$$\epsilon(p_z + p_F) = -\epsilon(p_z - p_F), \quad |p_z| < p_F \tag{1.3}$$

then (1.2) satisfies

$$\epsilon_{\vec{p}+\vec{q}_0/2} = -\tfrac{1}{2}\epsilon_{\vec{p}-\vec{q}_0/2}, \quad |p_z| < p_F \tag{1.4}$$

with

$$\vec{q}_0 = (\pi/a, \pi/a, 2p_F). \tag{1.5}$$

The condition (1.4) leads to perfect nesting of opposite sides of the Fermi surface in the q_0 direction so that the MF theory is formally the same as the 1-D MF theory. The instability corresponds to $\vec{q}_0$ which implies that CDW's on adjacent chains have opposite phases. This can be understood as if the system tries to minimize the variations in density by locating a density maximum near a density minimum on the neighboring chains.

The region of validity of this theory is limited by two effects: (i) Fluctuation effects which restrict the MF theory to the range

$$t_\perp \gtrsim 2T_P, \tag{1.6}$$

and (ii) deviation from Eq. (1.3) which for $\epsilon(p_z)$ given by the free-electron dispersion allows $T_P \neq 0$ in the range

$$t_\perp \lesssim 2(T_P T_F)^{1/2}, \tag{1.7}$$

where T_F is the Fermi temperature.

Since $T_P \ll T_F$, there is a large range of values for $t_\perp$ between Eqs. (1.6) and (1.7) for which a 1-D MF theory is effectively valid.

In the present work we are mainly concerned with the range (1.6)–(1.7) for the interchain coupling. Using the results for small interchain coupling,[14] more conclusions can be reached.

The summation of the most diverging diagrams is equivalent to the summation of effectively 1-D diagrams. Thus only the condition (1.4) is needed and the interchain coupling does not appear in the results. However, one should keep in mind the existence of the interchain coupling (1.2) which is needed explicitly in diagrams which are not effectively 1-D.

Preliminary results of the present investigation were published elsewhere.[17-19]

In Sec. II we extend the results of Ref. 16 to include all the couplings of Fig. 1 in the nonretarded limit. The summation of the most diverging diagrams turns out to be different from the parquet sum[10,11] and the conclusions are different too. The Peierls and superconducting phases can coexist only on one line which is again $s_1 = 2s_2$.

In Sec. III we consider the effect of a finite bare phonon frequency ω_0 on T_P. It is shown that the s_2 interaction is retarded and that T_P is a decreasing function of ω_0. This dependence becomes important for high frequencies $\omega_0 \gtrsim 2\pi T_P$. A positive isotope shift is predicted and may be observed experimentally if $\omega_0 \gtrsim 2\pi T_P$.

In Sec. IV T_P and T_s are compared in a system with a finite ω_0. It is shown that for a given ω_0 and s_2 there is a critical s_1 such that the Peierls instability dominates for higher s_1, while superconductivity dominates for lower s_1. Thus the Peierls instability imposes an upper limit on the temperatures T_s. The relevant parameters for obtaining higher transition temperatures T_s are discussed in Sec. V.

II. NONRETARDED INTERACTIONS

In this section we assume a nonretarded interaction between electrons as described by the couplings of Fig. 1. In what follows 1-D notation is used and $q_0 = 2p_F$. However, the interchain coupling is readily introduced by Eq. (1.2) since the condition (1.4) is the only restriction on the electron dispersion that we need.

The Hamiltonian of the system is

$$H=\sum{}'\epsilon_{p+q_0/2}(c^\dagger_{p+q_0/2\sigma}c_{p+q_0/2\sigma}-c^\dagger_{-p-q_0/2\sigma}c_{-p-q_0/2\sigma})+\frac{g_1}{2}\left(\sum{}'c^\dagger_{p_1+q_0/2\sigma}c_{p_4-q_0/2\sigma}c^\dagger_{p_2-q_0/2\sigma'}c_{p_3+q_0/2\sigma'}+\text{H.c.}\right)$$
$$+\frac{g_2}{2}\left(\sum{}'c^\dagger_{p_1+q_0/2\sigma}c_{p_4+q_0/2\sigma}c^\dagger_{p_2-q_0/2\sigma'}c_{p_3-q_0/2\sigma'}+\text{H.c.}\right)+\frac{g_3}{2}\left(\sum{}'c^\dagger_{p_1+q_0/2\sigma}c_{p_4-q_0/2\sigma}c^\dagger_{p_2+q_0/2\sigma'}c_{p_3-q_0/2\sigma'}+\text{H.c.}\right)$$
$$+\frac{g_4}{2}\left(\sum c^\dagger_{p_1+q_0/2\sigma}c_{p_4+q_0/2\sigma}c^\dagger_{p_2+q_0/2\sigma'}c_{p_3+q_0/2\sigma'}+(\tfrac{1}{2}q_0\to-\tfrac{1}{2}q_0)\right) \quad (2.1)$$

The prime on $\sum$ restricts momentum summation to $|p_i|<p_F$ and $p_1+p_2=p_3+p_4$. Summation includes also spins ($\sigma,\sigma'=\uparrow$ or $\downarrow$) and $c^\dagger_p$ is an electron creation operator.

The couplings g_2, g_4 represent scattering with a small momentum transfer while g_1 describes the large momentum ($\sim q_0$) transfer. For a half-filled band a momentum transfer of $4p_F=2\pi/c$ (c is the lattice constant along the chain) is possible and corresponds to the coupling g_3.

We use in this work the Nambu formalism for both superconductivity[20] and the Peierls phase.[21] Within this formalism the order parameters of both phases are easily handled.

In the Nambu formalism of superconductivity[20] the spinor field $\tilde\psi^\dagger_p=(c^\dagger_{p\uparrow}, c_{-p\downarrow})$ is introduced. Here we superimpose the Peierls-type correlation by defining the four-dimensional field

$$\psi^\dagger_p=(\tilde\psi^\dagger_{p+q_0/2}, \tilde\psi^\dagger_{p-q_0/2}), \quad |p|<p_F$$
$$=(c^\dagger_{p+q_0/2\uparrow}, c_{-p-q_0/2\downarrow}, c^\dagger_{p-q_0/2\uparrow}, c_{-p+q_0/2\downarrow}), \quad (2.2)$$

and ψ_p is the Hermitian-conjugated column vector.

The wave vector p is restricted by $|p|<p_F$ so that the phase space includes momenta in the range $(-2p_F, 2p_F)$. This range is sufficient for us since the important states are near the Fermi surface $\pm p_F$ and correspond to $|p|\ll p_F$ in Eq. (2.2).

The 4×4 space is a direct product of the superconducting 2×2 space with σ_i as the Pauli matrices, and the Peierls 2×2 space with τ_i as the Pauli matrices. In what follows the direct products appear in this order.

The Hamiltonian [Eq. (2.1)] is now transformed into the following form:

$$H=\sum{}'\epsilon_{p+q_0/2}\psi^\dagger_p\sigma_3\tau_3\psi_p$$
$$+\sum_{i=1}^{4}\bar g_i\sum{}'\psi^\dagger_{p_1}\Gamma_i\psi_{p_4}\psi^\dagger_{p_2}\Gamma_i\psi_{p_3}, \quad (2.3)$$

where

$$\bar g_1=\tfrac14(g_1+g_3), \quad \Gamma_1=\sigma_3\tau_1,$$
$$\bar g_2=\tfrac14(g_1-g_3), \quad \Gamma_2=\sigma_3\tau_2,$$
$$\bar g_3=\tfrac14(g_2+g_4), \quad \Gamma_3=\sigma_3 1, \quad (2.4)$$
$$\bar g_4=\tfrac14(g_4-g_2), \quad \Gamma_4=1\tau_3.$$

The Green's function in the Matsubara formalism [$\omega_n=\pi T(2n+1)$] is a 4×4 matrix

$$G^{-1}(p,i\omega_n)=i\omega_n 11-\epsilon_{p+q_0/2}\sigma_3\tau_3-\Sigma(p,i\omega_n). \quad (2.5)$$

The self-mass $\Sigma(p,i\omega_n)$ can be expanded in the 16 basis matrices. The various coefficients Δ_i in this expansion are the order parameters of the possible instabilities. In Ref. 17 it was shown that there are seven possible types of instabilities. Here we are interested with only two of these. Superconductivity (singlet pairing) corresponds to a correlation $\langle c^\dagger_{p_F\uparrow}c^\dagger_{-p_F\downarrow}\rangle$ and is antisymmetric under spin reversal. Thus Δ_s is the coefficient of $\sigma_1 1$ or $\sigma_2 1$. The Peierls instability corresponds to $\langle c^\dagger_{p_F\uparrow}c_{-p_F\uparrow}\rangle$ and is symmetric under spin reversal. Thus Δ_p is the coefficient of $\sigma_3\tau_1$ or $\sigma_3\tau_2$. The self-mass is (up to the replacements $\sigma_1\to\sigma_2$ or $\tau_1\to\tau_2$)

$$\Sigma=\Delta_s\sigma_1 1+\Delta_p\sigma_3\tau_1. \quad (2.6)$$

In general, Δ_s and Δ_p are dependent on p and ω_n. The Green's function from Eqs. (2.5) and (2.6) is

$$G(p,i\omega_n)=-\frac{i\omega_n 11+\epsilon_{p+q_0/2}\sigma_3\tau_3+\Delta_s\sigma_1 1+\Delta_p\sigma_3\tau_1}{\omega_n^2+\epsilon^2_{p+q_0/2}+\Delta_s^2+\Delta_p^2}. \quad (2.7)$$

The next step is to obtain the equation of state with the effectively 1-D diagrams. As shown later on this amounts to the diagrams of Fig. 2 in the Nambu space. Using the usual rules of perturbation theory[20] we obtain

$$\Sigma(p,i\omega_n)=T\sum_{i=1}^{4}\left(\bar g_i\Gamma_i\sum_{k,m}\mathrm{Tr}[G(k,i\omega_m)\Gamma_i]-\bar g_i\Gamma_i\sum_{k,m}G(k,i\omega_m)\Gamma_i\right). \quad (2.8)$$

Comparing coefficients of various matrices in Eqs. (2.6) and (2.8) and summing over ω_m give

$$\Delta_p=-\Delta_p(2g_1-g_2+g_3)N(0)I[(\Delta_s^2+\Delta_p^2)^{1/2}], \quad (2.9)$$

$$\Delta_s=-\Delta_s(g_1+g_2)N(0)I[(\Delta_s^2+\Delta_p^2)^{1/2}], \quad (2.10)$$

where

$$I(\Delta)=\int d\epsilon\frac{\tanh[(\epsilon^2+\Delta^2)^{1/2}/2T]}{8(\epsilon^2+\Delta^2)^{1/2}}. \quad (2.11)$$

The replacements $\sigma_1\to\sigma_2$ or $\tau_1\to\tau_2$ in Eq. (2.6)

imply a phase change in the order parameters. If σ_2 replaces σ_1, there is no change in Eqs. (2.9) and (2.10). However, if τ_2 replaces τ_1, g_3 in Eq. (2.9) changes sign, and the possibility with $|g_3|$ dominates. Now $g_3 \neq 0$ means that q_0 is commensurate with the lattice so that commensurability determines the phase of the CDW. This leads to pinning of the CDW which is a well-known effect.[22]

Equations (2.9) and (2.10) give nonzero solutions for both Δ_p and Δ_s only on the line

$$s_1 = 2s_2 - |s_3|, \tag{2.12}$$

where Eq. (1.1) is used and also $s_3 = -g_3 N(0)$.

Outside the line (2.12) only one of the order parameters can exist, either superconductivity for $s_1 < 2s_2 - |s_3|$ or the Peierls phase for $s_1 > 2s_2 - |s_3|$. This incompatibility of the two phases was noted by Levin *et al.*[23] However, their results do not account for the specific role of the s_2 coupling.

Both phases lead to gaps at the Fermi level so that the density of states at $\epsilon = 0$ vanishes. Thus the appearance of one of the phases eliminates the other phase. A demonstration of this effect is provided by pressure experiments on $NbSe_2$.[24] In this and other similar compounds CDW's appear at T_{CDW} due to nesting of parts of the Fermi surface, and superconductivity may appear at lower temperatures T_s. As pressure increases T_{CDW} is lowered but T_s is raised. The pressure distorts the Fermi surface, lowers T_{CDW}, the density of states near $\epsilon = 0$ is increased, and so T_s is raised. If the whole Fermi surface were involved in creating the CDW, then superconductivity at lower temperatures would be eliminated, as is the case with KCP and TTF-TCNQ.

The effect of g_3 as seen from Eqs. (2.9) and (2.12) is to increase T_P and reduce the range of parameters which allow T_s. Thus higher transition temperatures T_s are available for the incommensurate case with $g_3 = 0$.

In the following we concentrate on the couplings s_1 and s_2 and assume $g_3 = 0$. The transition temperatures are obtained by

$$I(\Delta = 0) = \tfrac{1}{4} \ln(1.13 E_c / T), \tag{2.13}$$

where E_c is an energy cutoff of the order of T_F,[16]

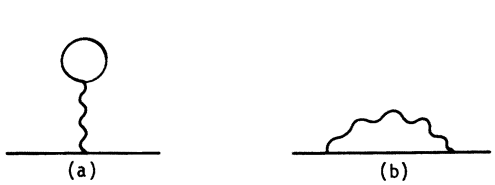

FIG. 2. Electron self-mass corrections: (a) Direct term. (b) Exchange term. Electron lines are in a 4×4 (Sec. II) or 2×2 (Secs. III and IV) Nambu representation.

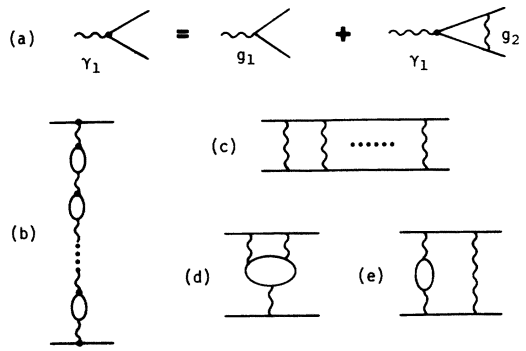

FIG. 3. (a) Equation for vertex corrections. (b) Peierls channel. (c) Superconducting channel. (d) and (e) An effect of the superconducting channel on the Peierls channel (d), and vice versa (e).

and Eq. (2.13) is valid for $T \ll E_c$. From Eqs. (2.9) and (2.10),

$$T_P = 1.13 E_c \exp[-4/(2s_1 - s_2)], \tag{2.14}$$

$$T_s = 1.13 E_c \exp[-4/(s_1 + s_2)]. \tag{2.15}$$

Let us now analyze the diagrams of Fig. 2 and check other types of diagrams. By iterating the exchange term in the direct term of Fig. 2 it is seen that vertex corrections of the ladder type are involved. These are shown in Fig. 3(a) and are given by the equation

$$\gamma_1 = g_1 - T \sum_{p,m} \gamma_1 G(p, i\omega_m) G(p + q_0, i\omega_m) g_2, \tag{2.16}$$

γ_1 is the renormalized vertex with transfer of $q = q_0$ and $\omega = 0$. Here $G^{-1}(p, i\omega_m) = i\omega_m - \epsilon_p$ is the Green's function in the metallic phase. The important contribution in Eq. (2.16) comes from $p \simeq -p_F$ so that $p + q_0 \simeq p_F$. The same reasoning applies to the external legs so that only the interaction g_2 is involved in the renormalization (2.16). We define

$$I(T) = \frac{-T}{N(0)} \sum_{p,m} G(p, i\omega_m) G(p + q_0, i\omega_m). \tag{2.17}$$

By using Eq. (1.4) this is the same function (2.13) in the metallic phase, $\Delta = 0$. The solution of Eq. (2.16) is

$$\gamma_1 = g_1 / [1 - g_2 N(0) I(T)]. \tag{2.18}$$

The Peierls instability corresponds to the instability of the full interaction with momentum transfer of q_0. This is shown in Fig. 3(b) and is given by

$$\sim g_1 / [1 + 2\gamma_1 N(0) I(T)]\ . \tag{2.19}$$

Using Eqs. (2.18) and (2.13), a pole appears in Eq. (2.19) at the temperature (2.14). Thus the Peierls

channel of Figs. 3(a) and 3(b) is equivalent to Fig. 2 in the Nambu space. On the other hand, the superconducting channel of Fig. 3(c) leads to T_s of Eq. (2.15).

Our next step is to show that Figs. 3(a)–3(c) are more important then any other diagrams. The demonstration is based on the concept of effective one dimensionality. We have seen in the introduction and in more detail in Ref. 16 that the interchain coupling (2.2) leads to perfect nesting in the $\vec{q}_0$ direction. Diagrams which involve only two electron lines at one time (or within the same integral) with relative momentum q_0 give the 1-D result. This is due to the accumulation of the Kohn effect[25] on the whole Fermi surface with the same wave vector $\vec{q}_0$. The effective one dimensionality is evident also from the results (2.9) and (2.10) which do not depend on the interchain coupling, and only the relation (1.4) is needed.

Diagrams which involve more than two electrons in the same integration feel the nonplanarity of the Fermi surface and are therefore less divergent than in the 1-D case. For example Figs. 3(d) and 3(e) behave like $s^3\ln^2 T$ as $T\to 0$ in the 1-D case, so that they are equally divergent as the diagrams in Figs. 3(b) and 3(c). Figures 3(d) and 3(e) are the lowest-order corrections of the parquet approximation[10] which are not included in Figs. 3(b) and 3(c). These corrections represent the effect of the divergence in the superconducting channel on the Peierls channel [3(d)] and vice versa [3(e)]. When the interchain coupling $t_\perp$ is finite, Figs. 3(d) and 3(e) depend on both $t_\perp$ and the temperature (or energy cutoff[11]) T. The explicit dependence is rather complicated, but we are interested here in the type of divergence as $T\to 0$. For $T\gg t_\perp$ the 1-D form $s^3\ln^2 T$ is valid; however, for $T\to 0$ (or $T\ll t_\perp$) these diagrams become less divergent and behave like $s^3\ln T\ln t_\perp$. Thus the three dimensionality of the system decouples the superconducting and Peierls channels. The summation of most divergent diagrams which gives the parquet sum in the 1-D case reduces to Figs. 3(a)–3(c) when $t_\perp\neq 0$. These are the effectively 1-D diagrams with the results (2.14) and (2.15).

Practically, these results are reasonable when the interchain coupling is large enough [Eq. (1.6)]. When $t_\perp$ is smaller, diagrams like 3(d) and 3(e) become important. It turns out that these two diagrams give equal results. Since they represent the mutual effect between the superconducting and Peierls channels, it is plausible that reducing $t_\perp$ will reduce T_P and T_s by the same amount so that the coexistence line remains $s_1=2s_2$. This conjecture is strengthened by the 1-D results[12,13] and the results[14] for small $t_\perp$, as discussed above.

III. RETARDED INTERACTIONS

Attractive interactions between electrons are due to the retarded electron-phonon interaction. The results of Sec. II are valid when the bare phonon frequency is large $\omega_0\gg E_c$ so that E_c is the only energy cutoff in the problem. The effects of a finite ω_0(or $\omega_0<E_c$) on T_s are well known,[20] and we concentrate in this section with the effects on T_P.

We start from the Fröhlich Hamiltonian[20] which includes the g_1 and $g_2=g_4$ type interactions of Fig. 1:

$$H=\sum_p \epsilon_p c_p^\dagger c_p+\sum_q \omega_q^0 a_q^\dagger a_q+\sum_{p,q} ig_q\varphi_q c_{p+q}^\dagger c_p, \tag{3.1}$$

where $a_q^\dagger$ is a phonon creation operator $\varphi_q=a_q+a_{-q}^\dagger$ and g_q is the electron-phonon coupling constant.

We define spinors in the Peierls space

$$\psi_p^\dagger=(c_{p+q_0/2}^\dagger c_{p-q_0/2}^\dagger),\quad |p|<p_F. \tag{3.2}$$

We also need the phase (ϕ) and amplitude (R) phonon operators[21,22]

$$\begin{aligned} a_\phi(q)&=(a_{q_0+q}-a_{-q_0+q})/i\sqrt{2}\,,\\ a_R(q)&=(a_{q_0+q}+a_{-q_0+q})/\sqrt{2}\,, \end{aligned}\quad |q|<p_F \tag{3.3}$$

and the phonon fields

$$\begin{aligned} \phi_q&=a_\phi(q)+a_\phi^\dagger(-q),\\ R_q&=a_R(q)+a_R^\dagger(-q). \end{aligned} \tag{3.4}$$

Using Eq. (1.4) the Hamiltonian (3.1) is now written in the form

$$\begin{aligned} H=&\sum{}' \epsilon_{p+q_0/2}\psi_p^\dagger\tau_3\psi_p+\sum{}' \omega_q^0 a_q^\dagger a_q\\ &+\sum{}' \omega_0[a_\phi^\dagger(q)a_\phi(q)+a_R^\dagger(q)a_R(q)]\\ &-\frac{g}{\sqrt{2}}\sum{}' \phi_{p'-p}\psi_{p'}^\dagger\tau_1\psi_p-\frac{g}{\sqrt{2}}\sum{}' R_{p'-p}\psi_{p'}^\dagger\tau_2\psi_p\\ &+\sum{}' ig_{p'-p}\varphi_{p'-p}\psi_{p'}^\dagger 1\psi_p. \end{aligned} \tag{3.5}$$

We assume $\omega_{q_0\pm q}=\omega_0$ and $g_{q_0+p'-p}=g$ since the important states have $|q|$, $|p|$, and $|p'|\ll p_F$. We also use $g_q=-g_{-q}$.[20] The last term in Eq. (3.5) is the interaction of phonons φ_q with small momenta.

The electron self-mass has now the general form

$$\Sigma(p,i\omega_n)=i\omega_n[1-Z_n(p)]\underline{1}+\chi_n(p)\tau_3+\Delta_n(p)\tau_2. \tag{3.6}$$

The order parameter $\Delta_n(p)$ represents a finite expectation value of the amplitude mode, and according to Eq. (3.5) is a coefficient of τ_2. (The replacement $\tau_2\to\tau_1$ would merely exchange the interpretations of the ϕ and R modes.)

We proceed to evaluate $\Sigma(i\omega_n,p)$ using Fig. 2, and the interactions now are the various phonons of (3.5),

$$\Sigma(p, i\omega_n) = g^2 T \sum{}' \tau_2 \mathrm{Tr}[G(p', i\omega_m)\tau_2] D_0(q_0, 0) - \frac{g^2}{2} T \sum{}' \tau_1 G(p', i\omega_m)\tau_1 D_\phi(p - p', i\nu_{n-m}) - \frac{g^2}{2} T \sum{}' \tau_2 G(p', i\omega_m)\tau_2 D_R(p - p', i\nu_{n-m}) - g_0^2 T \sum{}' 1 G(p', i\omega_m) 1 D_\varphi(p - p', i\nu_{n-m}), \tag{3.7}$$

where $D_{\phi,R,\varphi}$ are the propagators of the various phonons, $\nu_n = 2\pi T_n$, and g_0 is the coupling of the small-momentum phonons with the electrons. The direct term of Fig. 2 couples only the R mode and gives the first term of Eq. (3.7). By iterating the direct term on itself it is seen that the phonon self-mass corrections are already included so that the bare phonon propagator must be used

$$D_0(q, i\nu_n) = -2\omega_0/(\nu_n^2 + \omega_0^2). \tag{3.8}$$

We assume that the phonon frequency ω_0 does not depend on the momentum. This is reasonable near q_0 and for all momenta for an optical phonon. For acoustic modes (which must be three dimensional near $q = 0$ to maintain the lattice) the phonons with momenta $q_z \sim 0$ contribute mainly when the transverse momenta q_x, q_y are large[26] (higher-density of states), and then $\omega_0(q)$ is approximately constant. Thus we assume a constant ω_0 and also expect $s_1 \simeq s_2$.

Comparing coefficients of the various matrices in Eqs. (3.7) and (3.6) gives the equations for Δ, Z, and χ. The corrections Z and χ do not belong to Figs. 3(a) and 3(b) and are not effectively 1-D. Z and χ represent the electron self-mass corrections in the normal (metallic) phase and give a diverging result when $t_\perp \to 0$. It was shown in Ref. 19 that the diverging term can be neglected for large enough $t_\perp$, as given by Eq. (1.6). Thus we use $Z = 1$ and $\chi = 0$, and the gap equation becomes

$$\Delta_n(p) = T \sum_{p',m}{}' \frac{\Delta_m(p')}{\omega_m^2 + \epsilon^2_{p'+q_0/2} + \Delta_m^2(p')} \left[-2g^2 D_0(q_0, 0) - \tfrac{1}{2} g^2 D_\phi(p - p', i\nu_{n-m}) + \tfrac{1}{2} g^2 D_R(p - p', i\nu_{n-m}) + g_0^2 D(p - p', i\nu_{n-m})\right]. \tag{3.9}$$

At $T = T_P$ the phase and amplitude modes are degenerate so that D_ϕ and D_R are cancelled in (3.9). Thus the exchange term of Fig. 2 contributes only via the phonons φ with small momenta. This is precisely the analog of Fig. 3(a) where the vertex g_1 is renormalized only by the interactions g_2.

The phonon renormalizations are important mainly for phonons with momentum $\sim q_0$ so that for D_φ the bare propagator (3.8) may be used. In fact, the self-mass insertions for the φ phonons lead to diagrams which are not effectively 1-D, and thus should be avoided.

The couplings (1.1) are defined here by

$$g^2 = s_1\omega_0/2N(0), \qquad g_0^2 = s_2\omega_0/2N(0). \tag{3.10}$$

The equation for T_P is obtained by linearizing (3.9). Using $\Delta(\omega_m) = \Delta(-\omega_m)$ and integrating ϵ give

$$\Delta_n = \sum_{m=0}^{\infty} a_m(s_1 - s_2 b_{n,m})\Delta_m, \tag{3.11}$$

where

$$a_m = \frac{2\tan^{-1}(E_c/\omega_m)}{\pi(2m+1)}, \tag{3.12}$$

$$b_{n,m} = -\tfrac{1}{8}[D_0(i\nu_{n-m}) + D_0(i\nu_{n+m+1})]\omega_0. \tag{3.13}$$

For $T \ll E_c$ we can use Eq. (2.13) to obtain

$$\sigma \equiv \sum_{m=0}^{\infty} a_m = \tfrac{1}{2}\ln(1.13E_c/T). \tag{3.14}$$

For $s_2 = 0$ Eq. (3.11) is solved by

$$T_P^0 = 1.13E_c \exp(-2/s_1). \tag{3.15}$$

This is the usual MF result[16] when only the coupling s_1 is retained.

The coupling s_1 is responsible for the static distortion, hence the s_1 term in Eq. (3.11) is nonretarded. The dependence on ω_0 appears through the virtual processes of the exchange term—the s_2 term in Eq. (3.11).

When $\omega_0/T \to 0$ the repulsive s_2 term is minimal, and in this limit $b_{n,m} = \frac{1}{4}\delta_{n,m}$. For $s_2 \lesssim 1$, Eq. (3.11) is solved by

$$T_P^1 \simeq 1.13E_c \exp(-2/s_1 - \tfrac{1}{16}\pi^2 s_2), \tag{3.16}$$

so that the coupling s_2 reduces slightly the transition temperature. For $\omega_0 \to \infty$, $b_{n,m} \to \frac{1}{2}$ and Eq. (3.11) is again of the BCS type with the result

$$T_P^2 = 1.13E_c \exp[-4/(2s_1 - s_2)], \tag{3.17}$$

which is identical with Eq. (2.14). Thus for $s_1 \simeq s_2$ the coupling s_2 reduces the transition temperature drastically.

For a finite ω_0, T_P lies between the limits (3.16) and (3.17). Owing to the large energy cutoff E_c, it

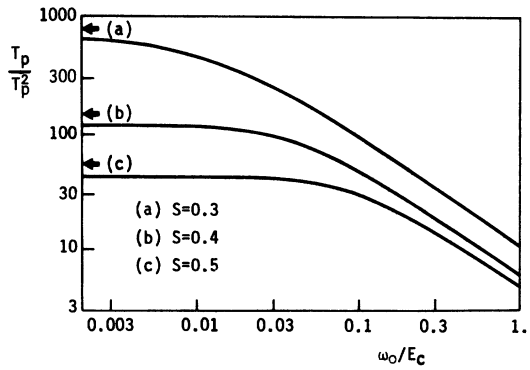

FIG. 4. T_P for $s_1 = s_2 = s$. For $\omega_0 \gg E_0$, T_P approaches the nonretarded result T_P^2 [Eq. (3.17)]. Arrows show the transition temperature for $s_1 = s$, $s_2 = 0$ [T_p^0 of Eq. (3.15)].

is advantageous to use Eq. (3.14). By iterating Eq. (3.11) a gap equation of the form

$$\sum_{m=0}^{\infty} A_{n,m}\bar{\Delta}_m = 0$$

is obtained, where $\bar{\Delta}_m = \sqrt{a_m}\,\Delta_m$ and

$$A_{n,m} = (\delta_{n,m} + s_2 a_{n,m} b_{n,m})(1 - s_1\sigma) + s_1 s_2 a_{n,m} \sum_{k=0}^{\infty} a_K b_{k,m}, \tag{3.18}$$

$$a_{n,m} = (a_n a_m)^{1/2}. \tag{3.19}$$

T_P is the solution for $\det(A) = 0$. The results for $s_1 = s_2 = s$ are shown in Fig. 4. The overall change in T_P is by a factor of $\sim \exp(2/s)$ which is very large if s is small.

The isotope shift parameter is defined by

$$\alpha = \frac{d\ln T_P}{d\ln M}, \tag{3.20}$$

where M is the effective mass of the vibration ω_0 $\sim M^{-1/2}$. Evidently $\alpha > 0$ and can be rather large

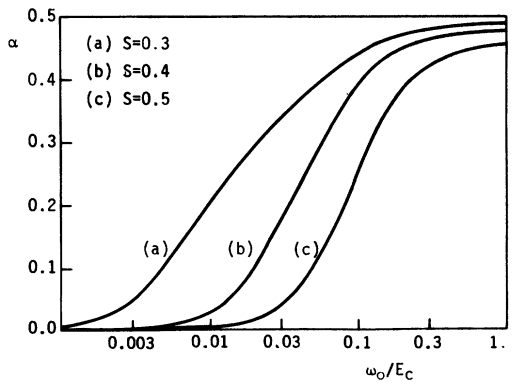

FIG. 5. Isotope shift parameter for $s_1 = s_2 = s$. For $\omega_0 \gg E_c$ the curves approach $\alpha = \frac{1}{2}/(1 + \omega_0/E_c) \simeq E_c/2\omega_0$ [see Eq. (3.21)].

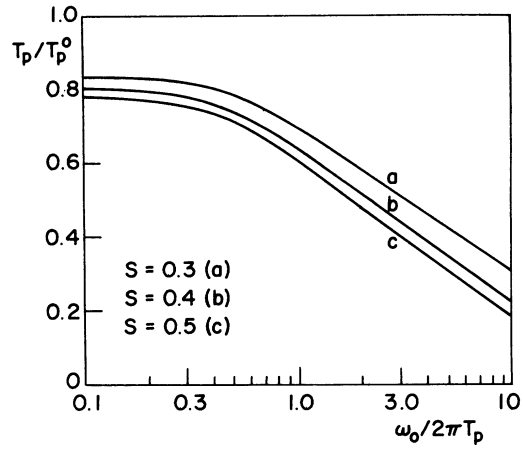

FIG. 6. T_P compared with T_P^0 [Eq. (3.15)] for $s_1 = s_2 = s$. Decrease in T_P becomes important for $\omega_0 \gtrsim 2\pi T_P$.

for high frequencies ω_0, as shown in Fig. 5.

In Figs. 6 and 7 we plot the results as functions of $\omega_0/2\pi T_P$. It is seen that this ratio is what mainly determines T_P/T_P^0 and α, and the dependence on s is much weaker.

Figure 6 can be used for an easy estimate of the coupling $s = s_1 = s_2$ from data on T_P, ω_0, and E_c. From the figure T_P^0 is estimated and then by Eq. (3.15) s_1 is evaluated. If $s_2 \neq s_1$, the reduction of T_P from T_P^0, and α, are both changed by roughly a factor of s_2/s_1.

For example in TTF-TCNQ, if the C=C vibration with $\omega_0 = 1600\ \mathrm{cm}^{-1}$ is responsible for the instability at $T_P = 53\ ^\circ\mathrm{K}$, then from Fig. 6 $T_p^0 \simeq 175\ ^\circ\mathrm{K}$. For $E_c = 0.5$ eV we obtain from Eq. (3.15) $s_1 = s_2 \simeq 0.55$. Suppose that this vibration contributes only half of the coupling, and the acoustic phonon contributes the other half. Since the acoustic phonon has low frequency ($\omega_0 < 2\pi T_P$), its s_2 coupling is strongly retarded and can be neglected. Thus $s_2/s_1 \simeq 0.5$

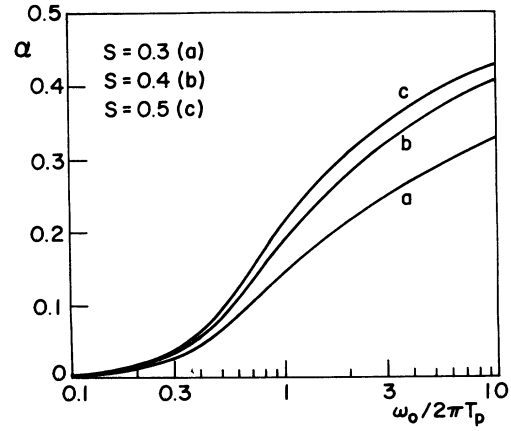

FIG. 7. Isotope shift parameter α for $s_1 = s_2 = s$. Shift is larger for $\omega_0 \gtrsim 2\pi T_P$.

and $T_P^0 \simeq 80$ K, $s_1 = 0.46$. If s_2 was ignored altogether, then $T_P^0 = T_P = 53$ °K and $s_1 = 0.42$. Thus the effects on the fitted value of the electron-phonon coupling are not very large. The more significant effect is in the isotope shift of T_P. This is further discussed in Sec. V. From Figs. 4–7 it is clear that retardation affects the results only for high-l frequency phonons such that $\omega_0 \gtrsim 2\pi T_P$.

In the solution of Eq. (3.18) matrices of dimensions larger than $\omega_0/2\pi T_P$ are needed. Generally matrices with dimensions 40–100 were used. For $\omega_0 > E_c$ solution of Eq. (3.18) is not practical, but then the gap equation on the real axis may be used. Using the same procedure as for superconductivity[27] and assuming a frequency-independent gap gives

$$T_P = T_P^2 (1 + E_c/\omega_0)^{s_2/(2s_1 - s_2)}. \tag{3.21}$$

The nonretarded results T_P^2 are obtained only for $\omega_0 \gg E_c$. Since usually $\omega_0 < E_c$, this demonstrates the importance of keeping both energies ω_0 and E_c in the problem.

An interesting feature of the gap equation (3.9) is that for $T < T_P$ the contributions of the phase and amplitude modes do not cancel. Since the corresponding frequencies satisfy[22] $\omega_\phi < \omega_R$, the term $D_R - D_\phi$ gives an attractive interaction. Thus the gap at $T = 0$ is larger than expected from a BCS-type equation, namely $2\Delta_0/T_P > 3.5$. This may explain some of the experimental observations which give $2\Delta_0/T_P = 8-10$.[7] This point was further discussed in Ref. 18.

In conclusion we have seen that T_P is a decreasing function of ω_0 due to the coupling s_2. This general feature is due to two factors: (i) The s_1 interaction is attractive while s_2 is repulsive. (ii) Retardation affects only the s_2 term. The factor (i) is true also in the soluble cases of the nonretarded interaction.[12] The factor (ii) is due to the coupling of s_1 to the static deformation, while s_2 couples only virtual phonons. Thus it can be expected that the general feature of the results will not change even for small interchain couplings, when summation of more diagrams is needed.

IV. SUPERCONDUCTIVITY AND PEIERLS INSTABILITY

Superconductivity is due to virtual phonons [Fig. 3(c)] so that retardation effects are essential for the calculation of the transition temperature T_s.

In systems with a spherical Fermi surface Migdal's theorem[20] enables us to neglect vertex corrections. Thus inclusion of electron and phonon self-mass corrections is sufficient and lead to the well-known Eliashberg equations for superconductivity.[20,26-28] However, if the Peierls channel diverges, vertex corrections appear which are equally important as the self-mass corrections. For example, Fig. 3(e) of a phonon self-mass correction in the superconducting channel is equal to the vertex correction implied by Fig. 3(d) (even for $t_\perp \neq 0$). We have seen in Sec. II that Figs. 3(d) and 3(e), are less divergent than Figs. 3(a)–3(c). Thus if we use the Eliashberg equations (which have no vertex corrections), we must also neglect the self-mass corrections. These are the Z and χ terms of Eq. (3.6) which were also neglected in the calculation of T_P. This approximation amounts to summation of the most divergent diagrams which for the superconducting channel are shown in Fig. 3(c). Thus the equation for the superconducting gap $\Phi_n(p)$ at $T = T_s$ is[27,28]

$$\Phi_n(p) = -T \sum_{p',m} \frac{1}{\omega_m^2 + \epsilon_{p'}^2} g_{p,-p'}^2 D_0(p - p', i\nu_{n-m}) \Phi_m(p'). \tag{4.1}$$

In Ref. 19 this equation was solved including the self-mass corrections. The numerical results turn out to be close to what we obtain in this section for large enough interchain couplings [Eq. (1.6)]. This confirms our claim that summation of most diverging diagrams is a good approximation, at least in the range (1.6). We emphasize that Eq. (4.1) does not include the self-mass corrections, which is consistent with neglecting vertex corrections.

Integrating $\epsilon_{p'}$ in Eq. (4.1) and using $\Phi(\omega_m) = \Phi(-\omega_m)$ give an equation of the form

$$\sum_{m=0}^{\infty} B_{n,m} \bar{\Phi}_m = 0$$

where $\bar{\Phi}_m = \sqrt{a_m}\, \Phi_m$. B is a symmetric matrix defined by using Eqs. (3.18) and (3.19)

$$B_{n,m} = \delta_{n,m} - (s_1 + s_2) a_{n,m} b_{n,m}. \tag{4.2}$$

T_s is the solution for $\det(B) = 0$. For $\omega_0 \gg E_c$ the nonretarded solution (2.15) is obtained. Usually $\omega_0 < E_c$ and the effects of retardation are important. As $\omega_0 \to 0$ the solution also satisfies $T_s \to 0$.

Solutions of Eq. (4.2) were done using matrices with dimensions 40–100. For $T/\omega_0 \lesssim 10^{-3}$ numerical solutions of Eq. (4.2) are not practical. However for $T \ll \omega_0$, ω_0 is in fact the energy cutoff in Eq. (4.4) and the BCS solution can be used

$$T_s \simeq 1.13\omega_0 \exp[-4/(s_1 + s_2)], \quad (T_s \ll \omega_0). \tag{4.3}$$

The solutions of T_s, T_P as functions of $s = s_1 = s_2$ are shown in Fig. 8. As ω_0 becomes higher the solutions for T_s increase towards the broken line C while the solutions for T_P decrease towards the full line C. For a given ω_0, T_s dominates below a critical value $s_c(\omega_0)$ while T_P dominates for stronger couplings. The critical value $s_c(\omega_0)$ in-

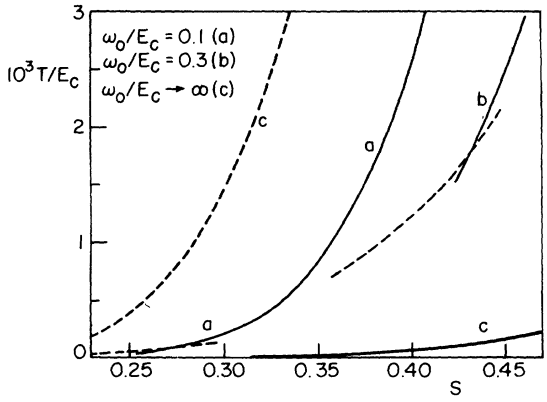

FIG. 8. T_P (full lines) and T_s (broken lines) for $s_1 = s_2 = s$.

creases with ω_0 and so do the available temperatures T_s.

The critical values of the couplings s_1, s_2 are shown in Fig. 9. These lines are the coexistence curves on which $T_s = T_P$. The lines determine an upper bound on the temperatures T_s, since beyond the lines the Peierls instability dominates. These maximal temperatures T_s are shown in Fig. 10.

These results determine the important parameters for obtaining a higher T_s: (i) Higher frequencies ω_0. (ii) Stronger coupling s_2 (although for s_2 too large a martensitic-type instability might appear[17]). (iii) Stronger coupling s_1, but below the critical curve of Fig. 9. For $s_2 = 1$ we obtain from Fig. 10 $\max(T_s) \simeq \frac{1}{20}\omega_0$, a result which demonstrates the importance of increasing ω_0.

In view of the discussion in Sec. II it is possible that the phase diagram of Fig. 9 is valid also for interchain couplings smaller than Eq. (1.6) when more diagrams are needed. However, the temperatures of Fig. 10 will decrease if $t_\perp$ becomes smaller. This is, of course, undesirable if we wish to obtain a higher T_s.

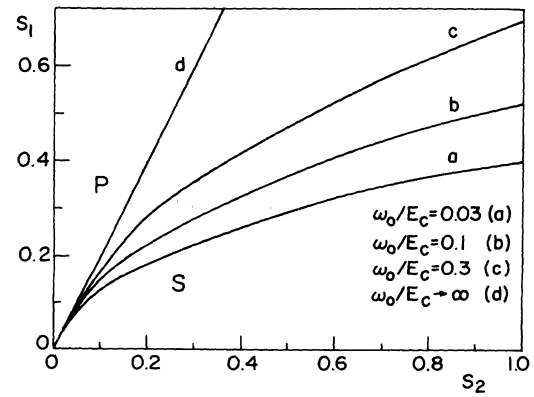

FIG. 9. Coexistence curves between the superconducting phase (S) and the Peierls phase (P).

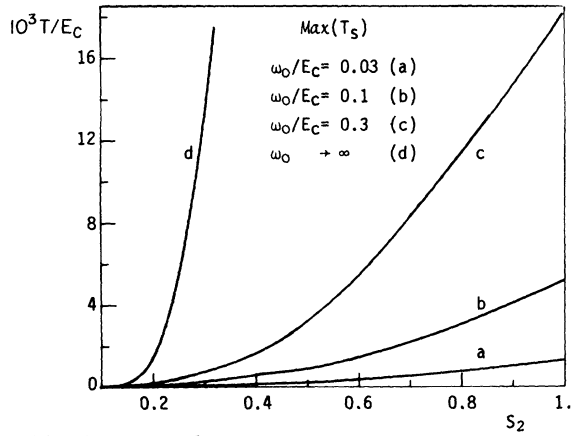

FIG. 10. Maximal transition temperatures for superconductivity which correspond to the coexistence curves of Fig. 9. For $s_2 = 1$, $\max(T_s) \simeq \frac{1}{20}\omega_0$.

The Peierls instability prevents us from obtaining higher temperatures T_s. This is an example of the well-known harmful effect of lattice instabilities on superconductivity.[29] There is a possibility to bypass the difficulty by eliminating the Peierls instability. This is possible by increasing the interchain coupling beyond the critical coupling [Eq. (1.7)], i.e., by applying pressure. If the Peierls channel is not divergent, then vertex corrections [i.e., Fig. 3(d)] become less important than self-mass corrections [i.e., Fig. 3(e)]. In this case the Eliashberg equations, including self-mass corrections, can be used, as was done in Ref. 19. The results show that as $t_\perp$ approaches the critical $t_\perp$ [Eq. (1.7)] from above T_s is somewhat increased, an effect due to the appearance of soft phonons near the Peierls instability.

It has been claimed that phonons which are too soft (with frequency below $2\pi T_s$) are harmful to superconductivity. Bergman and Rainer[30] have shown that this claim is incorrect, as far as the Eliashberg equations are concerned. Their conclusion is that if we add phonons to the system T_s always increases, and this increase is stronger if the added phonons have frequency $\sim 2\pi T_s$. If we keep the number of phonons constant, $\int B(\omega)d\omega = \text{const.}$ [$B(\omega)$ is the phonon density of states for some q], then shifting phonons from a frequency $\sim 2\pi T_s$ to other frequencies will decrease T_s. However, in our case the number of phonons is not constant and in fact diverges as the Peierls instability is approached. The constant quantity in this case is the sum rule $\int_0^\infty \omega B(\omega)d\omega = \omega_0$. As the phonons become softer their number increases and the overall effect is to increase T_s.

This conclusion is valid only within the full Eliashberg equations. We again emphasize that if $T_P \neq 0$ is possible, then the divergence of the Peierls channel will lead to vertex corrections which will

probably cancel the effect of the soft phonons. In this case a self-consistent solution of the Eliashberg equations requires that the self-mass corrections should be neglected, and phonon softening has no effect on T_s.

V. DISCUSSION

In this work we developed a model which demonstrates the competition between superconductivity and the Peierls instability, including effects of retardation and interchain coupling.

Let us first examine the deficiencies of the model: (i) Only hopping type interchain coupling is included. (ii) The interchain coupling is assumed large enough [Eq. (1.6)]. (iii) Intrachain Coulomb interaction between electrons is neglected. (iv) Perfect nesting or the symmetry (1.4) is assumed.

The assumptions (i)–(iii) enable us to obtain higher values for T_s. As mentioned in Sec. I the hopping-type interchain coupling is essential for obtaining $T_s \neq 0$. Thus the results of Fig. 10 give the maximal T_s also in the sense that fluctuations have a small effect on T_s [assumptions (i), (ii)] and that repulsive Coulomb interactions between electrons are not included [assumptions (i, iii)].

The direct (intrachain) Coulomb interaction is nonretarded, so that its effect on T_P and T_s is included in Sec. II. Separating the contributions to the couplings s_1 and s_2 to electron-phonon type and electron-electron type, the effective s_1 of Sec. III [Eq. (3.11)] is $s_1(\text{el-ph}) + s_1(\text{el-el}) - \frac{1}{2}s_2(\text{el-el})$. Since long-range Coulomb coupling is both stronger and repulsive, ($s < 0$) T_p is enhanced. On the other hand, T_s is reduced by the direct Coulomb interaction.[27] Thus the effect of (iii) can be evaluated for a given system and will lead to a lower limit on the temperatures T_s.

The assumption (iv) was investigated in Ref. 16. It was shown there that deviations from the symmetry (1.4) become important only for large interchain couplings [Eq. (1.7)]. For smaller interchain couplings the exact symmetry (1.4) can be safely used even if symmetry breaking terms exist in the dispersion $\epsilon(p_z)$. Thus for not too large interchain couplings [Eq. (1.7)] the Peierls instability is unavoidable, and imposes an upper limit on the temperatures T_s.

Deviations from orthorhombic structure [as implied by Eq. (1.2)] lead to stronger next-nearest-neighbor coupling which breaks the symmetry (1.4). Eventually, for the hexagonal structure, each chain cannot have opposite phase to its six nearest chains. Therefore perfect nesting does not occur and suppressing the Peierls instability would be easier than in the orthorhombic structure.

For very low interchain couplings the 1-D results[11-15] could be a better starting point. However, we have demonstrated in this work the importance of including the interchain coupling, and more significantly the phonon frequency ω_0 when dealing with real systems. Thus our model is a reasonable basis for analyzing and predicting the behavior of actual systems.

We have shown that the important parameters which can lead to higher temperatures T_s are as follows: (a) Higher frequencies ω_0 (Fig. 10). (b) Stronger couplings s_1, s_2, but s_1 must be smaller than a critical value determined by s_2 and ω_0 (Fig. 9). Thus the increase of the long-range attractive interaction s_2 helps more than the increase of s_1. (c) The commensurate case with the coupling g_3 should be avoided. This coupling increases T_P but not T_s [Eqs. (2.9) and (2.10)] so that the coexistence curve [Eq. (2.12)] shifts to the right in Fig. 9 and the available temperatures T_s become lower. (d) If the Peierls phase can be eliminated, then it does not limit the temperatures T_s. This can be achieved by increasing the interchain coupling beyond the critical value (1.7), i.e., by pressure. Also the soft phonons help in this case.[19] The Peierls phase is suppressed also by nonmagnetic impurities.[31] However, experimentally it seems that T_P is not sensitive to impurities[1] so that this mechanism needs further study.

Our conclusions raise the question whether one dimensionality helps superconductivity at all. The conditions for higher ω_0 and stronger electron-phonon coupling lead to higher T_s in usual three dimensional systems,[32] and the Peierls phase does not interfere. The answer is that one dimensionality helps to raise T_s indirectly by providing systems with better parameters. The following mechanisms illustrate this point: (a) If the Fermi level is near the band edge, $N(0)$ is large and so the couplings (1.1) are stronger. (b) If the interchain coupling is larger but close to the critical value (1.7), the soft phonons help to raise T_s.[17] (c) Very high frequencies ω_0 are available as intramolecular bond vibrations in organic molecules, such as in TCNQ. Owing to the planar structure of these molecules, they form a crystal with a preferred direction along the stacking axis. Thus the search for high ω_0 leads us to quasi-1-D organic crystals.

The mechanisms (a) and (b) may account for the relatively high T_s of the $A15$ compounds.[4] But the mechanism (c) seems to be the most promising way for obtaining higher temperatures T_s.

Owing to the importance of the high-frequency phonons we suggest two methods for detecting the coupling of such phonons with electrons in the Peierls phase. The first method is by optical and Raman measurements. When $\omega_0 \gg T_p$, a high-frequency branch exists in addition to the soft mode.[33]

In the Peierls phase this high-frequency branch can be detected by both optical and Raman measurements.[33]

It was suggested that high-frequency intramolecular bond vibrations contribute to the Peierls instability in TTF-TCNQ.[33,34] A broad minimum in the reflectivity around 1500 cm^{-1} was fitted to the C≡N vibration with $\omega_0 = 2200$ cm^{-1} using $s \simeq 0.4$. However if s is shared among a few frequencies, the C=C vibration at $\omega_0 = 1600$ cm^{-1} may cause this minimum.

The second method for detecting high frequencies which couple to electrons is by measuring the isotope shift of T_p. If the C≡N is responsible for the transition in TTF-TCNQ, then Fig. 7 shows that the isotope ^{15}N would increase T_P by ~1%. If the C=C mode is the important vibration, then ^{13}C would increase T_P by ~3%. If these vibrations couple by s_i which is less than the total coupling s, then the isotope shifts are reduced by a factor of roughly s_i/s. If the total coupling s is distributed equally among many vibrations,[34] then ^{13}C which changes the frequency of most of the vibrations will shift T_P by (2–3)%. Experimentally the temperature T_P can be determined up to ±0.2%.[35] Thus the isotope shifts of T_P can be determined and verify whether high-frequency phonons indeed contribute significantly to the Peierls instability of TTF-TCNQ.

Another type of an important measurement is the pressure dependence of the Peierls phase. Pressure increases the interchain coupling, and above some critical pressure the Peierls instability is suppressed and superconductivity would appear. In KCP, measurements were carried up to 35 kbar.[36] A fit to the theory of Refs. 16 and 19 showed[36] that above 70 kbar the Peierls instability would be suppressed. Assuming that only the acoustic phonon is coupled, we expect superconductivity with $T_s = 1$–6 °K for pressures above 70 kbar.

High-pressure experiments on TTF-TCNQ may be even more interesting. Since high-frequency phonons may be important in this system, we may expect rather high values for T_s above the critical pressure.

A third type of a quasi-1-D conductor is the polymer $(SN)_x$,[8] with $T_s = 0.33$ °K. Indeed superconductivity dominates at such low temperatures according to Fig. 10. However, it is possible that the quasi-1-D nature of $(SN)_x$ is not intrinsic but due to the thin fibers which compose the crystal.[9] In such a case the interchain coupling can be rather large, and the Peierls instability is not possible.

Data on the strongly coupled phonons are important for determining the phase diagram (Fig. 9) and the maximal T_s (Fig. 10). If we assume that the acoustic phonons dominate in KCP and in TTF-TCNQ with $\omega_0 \sim 100$ °K, then at the corresponding temperatures $T_P \simeq 110$ or $= 53$ °K the Peierls instability indeed dominates, as evident from Fig. 10. However, if high-frequency phonons dominate in TTF-TCNQ, then this system may be rather close to the coexistence curve of Fig. 9. If so, a small decrease of the electron-phonon coupling (of s_1 in particular) would turn the system into a superconductor.

In conclusion, we have analyzed the various parameters and mechanisms which can lead to superconductivity at higher temperatures. Experiments on the available Peierls systems are suggested which may increase our knowledge on the important parameters for superconductivity.

ACKNOWLEDGMENTS

During the evolution of this work I have benefitted from discussions with H. Gutfreund, M. Weger, S. Alexander, A. Birnboim, D. Rainer, and D. J. Scalapino.

---

*Present address: Cornell University, Laboratory of Atomic and Solid State Physics, Clark Hall, Ithaca, N.Y. 14853.

[1]For reviews see, *Lecture Notes in Physics*, edited by H. G. Schuster (Springer, New York, 1975), Vol. 34.
[2]H. Fröhlich, Proc. R. Soc. A 223, 296 (1954).
[3]W. A. Little, Phys. Rev. 134, A1416 (1964).
[4]M. Weger, Rev. Mod. Phys. 36, 175 (1964); M. Weger and I. Goldberg, Solid State Phys. Vol. 28, 1 (1973).
[5]B. Renker, L. Pintschovius, W. Glaser, H. Rietschel, R. Comes, L. Liebert, and W. Drexel, Phys. Rev. Lett. 32, 836 (1974).
[6]F. Denoyer, R. Comes, A. F. Garito, and A. J. Heeger, Phys. Rev. Lett. 35, 445 (1975).
[7]S. Etemad, Phys. Rev. B 13, 2254 (1976).
[8]W. D. Gill, R. L. Greene, G. B. Street, and W. A. Little, Phys. Rev. Lett. 35, 1732 (1975).
[9]L. J. Azevedo, W. G. Clark, G. Deutscher, R. L. Greene, G. B. Street, and L. J. Suter, Solid State Commun. 19, 197 (1976).
[10]A. Bychkov, L. P. Gorkov, and I. E. Dzyaloshinskii, Zh. Eksp. Teor. Fiz. 50, 738 (1966) [Sov. Phys.-JETP 23, 489 (1966)].
[11]N. Menyhard and J. Solyom, J. Low Temp. Phys. 12, 529 (1973); J. Solyom, *ibid.* 12, 547 (1973).
[12]A. Luther and I. Peschel, Phys. Rev. B 9, 2911 (1974); E. H. Lieb and F. Y. Wu, Phys. Rev. Lett. 20, 1445 (1968); A. Luther and V. J. Emery, *ibid.* 33, 589 (1974).
[13]S. T. Chui and P. A. Lee, Phys. Rev. Lett. 35, 315 (1975); H. Gutfreund and B. A. Huberman (unpublished).
[14]R. Klemm and H. Gutfreund, Phys. Rev. B 14, 1086

(1976).
[15]L. Mihaly and J. Solyom, J. Low Temp. Phys. (to be published).
[16]B. Horovitz, H. Gutfreund, and M. Weger, Phys. Rev. B 12, 3174 (1975).
[17]B. Horovitz, Solid State Commun. 18, 445 (1976).
[18]B. Horovitz, Solid State Commun. 19, 1001 (1976).
[19]B. Horovitz and A. Birnboim, Solid State Commun. 19, 91 (1976).
[20]J. R. Schrieffer, in *Theory of Superconductivity*, edited by D. Pines (Benjamin, New York, 1964).
[21]H. G. Schuster, Phys. Rev. B 11, 613 (1975).
[22]P. A. Lee, T. M. Rice, and P. W. Anderson, Solid State Commun. 14, 703 (1974).
[23]K. Levin, D. L. Mills, and S. L. Cunningham, Solid State Commun. 15, 705 (1974).
[24]C. Berthier, P. Molinie, and D. Jerome, Solid State Commun. 18, 1393 (1976).
[25]W. Kohn, Phys. Rev. Lett. 2, 393 (1959).
[26]P. Morel and P. W. Anderson, Phys. Rev. 125, 1263 (1962).
[27]D. J. Scalapino, in *Superconductivity*, edited by R. D. Parks (Dekker, New York, 1969), p. 449.
[28]C. S. Owen and D. J. Scalapino, Physica 55, 691 (1971).
[29]B. T. Matthias, Physica 69, 54 (1973).
[30]G. Bergmann and D. Rainer, Z. Phys. 263, 59 (1973).
[31]H. G. Schuster, Solid State Commun. 14, 127 (1974).
[32]P. B. Allen and R. C. Dynes, J. Phys. C 8, L158 (1975).
[33]B. Horovitz, M. Weger and H. Gutfreund, Phys. Rev. B 9, 1246 (1974); J. Phys. C 7, 383 (1974); Solid State Commun. 15, 849 (1974); Phys. Rev. B 12, 1086 (1975).
[34]M. J. Rice, C. B. Duke, and N. O. Lipari, Solid State Commun. 17, 1089 (1975); M. J. Rice, Phys. Rev. Lett. 37, 36 (1976).
[35]P. M. Horn and D. Rimai, Phys. Rev. Lett. 36, 809 (1976).
[36]M. Thielemans, R. Deltour, D. Jerome, and J. R. Cooper, Solid State Commun. 19, 21 (1976).